

The effects of many-body interactions on point-defect generation *

S.P. Chou and N.M. Ghoniem

Mechanical, Aerospace and Nuclear Engineering Department, University of California, Los Angeles, California 90024-1597, USA

Point-defect generation by energetic displacement events is known to take place when a lattice atom acquires an energy several times its lattice binding value. In this energy range, many-body effects are important and interatomic pair potentials generally give poor representations of atomic interactions. By applying our newly developed molecular-dynamics code, CASC-MD, we investigate the influence of many-body interatomic interactions on the generation characteristics of point defects. We use a composite interatomic potential that assumes the pair-potential nature at high energies and the many-body nature, based on the embedded-atom formalism, at low energies. It is shown that many-body effects lead to lower directional sensitivity of the displacement threshold surface. For a 60 eV collision cascade in Cu, it is shown that the length of the replacement collision sequence decreases from 6 lattice constants at low temperature (near 0 K) to 1.5 lattice constants near the melting point.

1. Introduction

The generation of point defects has been studied theoretically by using both the Monte Carlo and the molecular dynamics (MD) methods with pair potentials for high energies [1–14]. Theoretical and experimental results both indicate that atomic displacements occur with a threshold energy on the order of a few times the lattice binding energy. Because pair potentials are generally inaccurate near the displacement threshold energy, the use of pair potentials to study this energy range is questionable. Daw and Baskes [15,16], using the embedded atom method (EAM), formulated the basis for a many-body potential by incorporating the embedding-function contribution to the atomic pair interaction. With a Taylor-series expansion about the equilibrium local electron density, Foiles [17] derived a many-body-type potential which accounts for the contribution of volume-dependent electron interactions. The EAM potential derived in this way is a good representation of atomic interactions in the sub- and low-eV energy range. Therefore, the cascade interaction is expected to be more precisely described by using a pure pair potential at high energies and the EAM many-body potential in the sub- and low-eV range.

In this work, the incorporation of both pair and many-body potentials into MD simulations is realized through the use of a composite spline technique. A brief discussion of the main features of a newly developed MD code, CASC-MD, is given. The collision-cascade interaction dynamics and calculations of the displacement threshold surface in copper are studied by using the Born–Mayer pair potential and comparing the results to the newly developed composite potential. Comparisons with earlier computer simulations by King and

Benedek [12–14] are then made. The effects of temperature on the length of the replacement collision sequence are also studied.

2. Development of CASC-MD

2.1. Spline potential

A molecular dynamics code, CASC-MD, has been developed to study low-energy collision cascades. The unique features of this code are the use of a more realistic potential for the description of atomic interactions and the incorporation of viscoelastic boundary conditions. A cubic-spline scheme is used to bridge the gap between the low-energy EAM many-body potential and the high-energy pair potential. The low-energy many-body potential for a solid at or near equilibrium is derived from the total energy of a system of atoms by using the EAM that is based on local density approximation. This many-body potential is derived by Daw et al. [15–17] and has the form

$$\phi_{\text{EAM}} = \phi_{ij}(R_{ij}) + 2 \frac{\partial F_i(\bar{\rho}^a)}{\partial \rho} \rho_{ij}^a(R_{ij}) + \frac{\partial^2 F_i(\bar{\rho}^a)}{\partial \rho^2} [\rho_{ij}^a(R_{ij})]^2, \quad (1)$$

where i and j are indices of interacting atoms, $\bar{\rho}^a$ is the local average background electron density on atom i , $\rho_{ij}^a(R_{ij})$ is the local average electron density contribution from atom j to atom i at a separation distance of R_{ij} , and ϕ_{ij} is the core–core repulsive potential between atoms i and j . The range of this potential extends to the third nearest neighbors.

The high-energy pair-interaction potential is well represented by the Ziegler potential [18]. The transition from high- to low-energy interactions is represented by a cubic-spline potential function which is adjusted to guarantee continuity of potential and force at two spline points, r_1 and r_2 , located along the interatomic sep-

* This work was supported by the US Department of Energy, Office of Fusion Energy, Grant #DE-FG03-84ER52110, with UCLA.

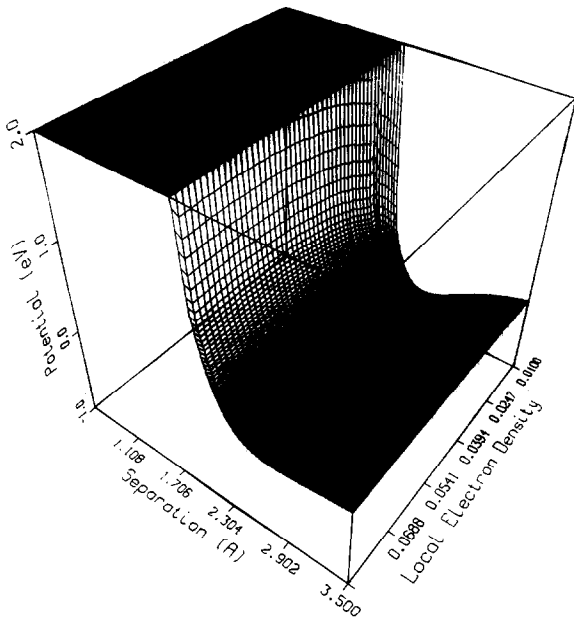


Fig. 1. Dependence of the composite potential on the interatomic separation distance and the local electron density.

aration distance. Details of the method are given in ref. [19]. Fig. 1 shows a 3D plot of the composite potential as a function of the distance between interacting atoms and the total local electron density for copper atoms. The transition region is taken to be from 1.5 to 2.0 Å. It is worth mentioning that the selection of r_1 and r_2 is achieved by requiring smooth force variation over the transition region. Improper choices of spline boundaries can artificially introduce high potential minima and maxima that locally trap recoils.

2.2. Molecular dynamics scheme and boundary conditions

In MD simulations, the motion of a system of particles can be fully described by the solutions of a system of Newtonian equations of motion (EOMs). EOMs are integrated using an explicit leapfrog technique (see ref. [19]).

In equilibrium MD simulations, it has been established that the dynamic behavior of a small number of atoms can be a valid statistical representation of the solid as long as periodic boundary conditions and velocity renormalization are used [20]. In equilibrium phase-transition problems, sample sizes of up to 250 000 atoms have been used. However, in our cascade simulations, we are not interested in simulating a global phenomenon (e.g., phase transitions) for which an increase in the size of the computational box is likely to give more accurate results. Rather, the size of the computational box is determined solely by the energy dissipation rate at the boundary. Ideally, and in an infinite solid, the excess kinetic energy of the primary knock-on atom

(PKA) must eventually be dissipated to the outside world or else it will lead to a uniform temperature rise. Practically, however, we are more interested in the study of energy dissipation in the generation of point defects. We introduce an arbitrary cutoff kinetic energy per atom (say, 1 eV), below which cascade simulation for the purpose of point-defect generation is no longer suitable. The number of atoms for a particular cascade simulation is chosen to guarantee that no energy reflection occurs at the boundary in a way that alters atomic rearrangements inside the computational box. We also introduce two atomic planes of special “boundary atoms” which have viscoelastic EOMs in order to simulate cascade energy dissipation into the surrounding solid. Details are given in ref. [19].

3. Low-energy collision-cascade simulations

The dynamics of a collision cascade by a 60 eV (speed = 135 Å/ps) Cu PKA initially along the [100] direction on a (001) plane in Cu at 300 K is illustrated in fig. 2. The X-axis is the particle ID number. It is arranged so that the particle ID number increases along the X-direction in the computational cell (boundary atoms are not included). It is clearly shown that the collision cascade subsides quickly in less than 0.15 ps, which is the collisional phase of the cascade evolution. None of the atoms has energy greater than 1 eV (17 Å/ps) at the end of this phase. It is observed that the energy propagation speed is greater than the speed of recoils and far exceeds the speed of sound. This is because the collective interaction is the dominant mode of energy transfer. Fig. 3 shows a linear replacement-

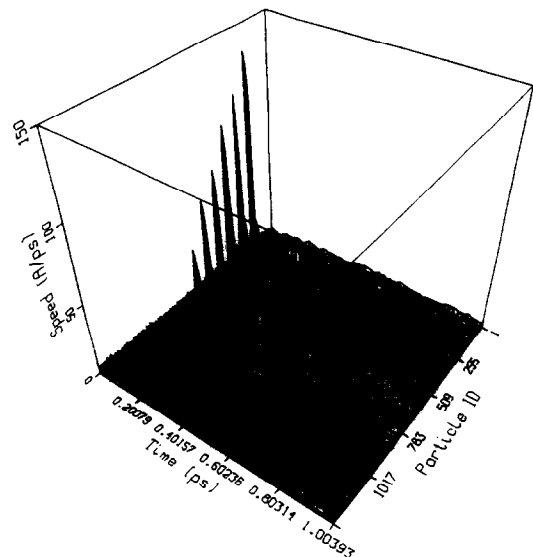


Fig. 2. Cascade dynamics of a 60 eV Cu PKA incident along the [100] direction in a (001) plane. The particle (recoil) ID number increases along the X-axis.

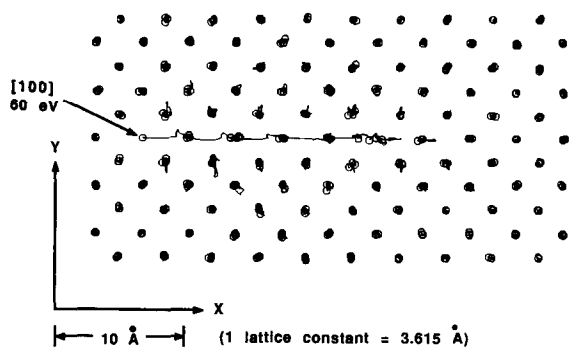


Fig. 3. Cascade trajectories for a 60 eV Cu PKA incident along the [100] direction in a (001) plane at 300 K. A linear RCS with a length of 5.5 lattice constants is produced.

collision sequence (RCS) generated by the same 60 eV Cu PKA in a layer, which has a thickness of 0.5 lattice constant, with the major interaction plane (001) in the middle. The linear RCS has a length of 5.5 lattice constants. The energy dissipation is preferred along special crystallographic directions (e.g., [100] and [110]). This is clearly shown by the larger-than-thermal vibration movement of the lattice atoms along these directions. Fig. 4 shows the effect of temperature on the RCS length by the same 60 eV PKA along the [100] direction. Cascade defocusing at high temperatures is clearly caused by variations of the impact parameter along the primary focusing direction which results in a shortening of the RCS length. In some cases, no displacement is generated at all. This suggests that the directional displacement threshold energy varies depending on the irradiation temperature. Fig. 5 shows CASC-MD calculations of the threshold displacement energy along selected crystallographic directions compared with the numerical results of King and Benedek [14]. For their numerical calculations, King and Benedek used the Born-Mayer pair potential. It appears that the use of

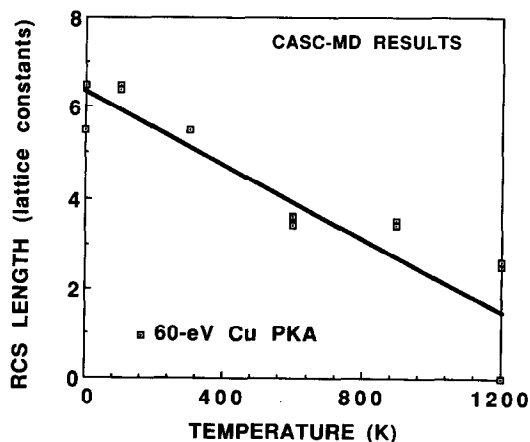


Fig. 4. The dependence of the linear RCS length on temperature.

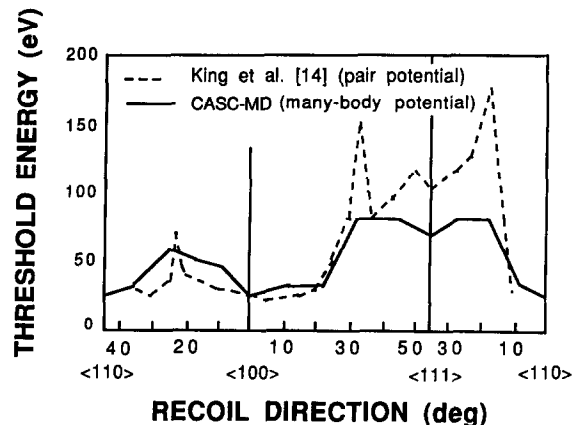


Fig. 5. A comparison between the displacement threshold energies along selected crystallographic directions evaluated by CASC-MD simulations and those of King and Benedek [14].

the present composite potential results in less sensitive directional variations of the displacement threshold when compared with the results of a pure pair potential. However, our computational results are more consistent with their experimental data on Cu [12–14].

4. Conclusions and future directions

In this work, a molecular dynamics code, CASC-MD, is developed. A composite potential (comprising pair- and many-body interaction types for high and low energies, respectively) is used and yields good agreements with experimental values for the displacement-threshold energy surface. Our results clearly show the influence of temperature on the dynamics of collision cascades and displacement generation. It is also shown that many-body effects are important to consider in the sub- and low-eV energy ranges.

Because of the complicated EAM potential at low energy and its long-range interactions, our analyses have been limited to small computational cells and sub-keV collision cascades. The computational overhead is a major concern for the use of such potentials: 15 min of CRAY-2 time for simulations of a computational cell size of 1271 particles with a duration of 1 ps. To extend our calculations to higher cascade energies and larger computational cells requires further development of the present code.

References

- [1] M. Yoshida, *J. Phys. Soc. Jpn.* 16 (1961) 44.
- [2] O. Oen and M.T. Robinson, *J. Appl. Phys.* 34 (1964) 2515.
- [3] T. Ishitani, R. Shimuzu and K. Murata, *Jpn. J. Appl. Phys.* 11 (1972) 125.
- [4] H.L. Heinisch, *J. Nucl. Mater.* 103&104 (1981) 1325; *J. Nucl. Mater.* 117 (1983) 46.
- [5] S.P. Chou and N.M. Ghoniem, *J. Nucl. Mater.* 117 (1983) 55.

- [6] J.B. Gibson, A.N. Goland, M. Milgram and G.H. Vineyard, *Phys. Rev.* 120 (1960) 1229
- [7] J.R. Beeler Jr., *Phys. Rev.* 150 (1966) 470.
- [8] R.N. Stuart, N.W. Guinan and B.J. Borg, *Radiat. Eff.* 30 (1976) 129.
- [9] J.D. Schiffgen and R.D. Bourquin, *J. Nucl. Mater.* 69 & 70 (1978) 790.
- [10] A. Tenenbaum and N.V. Doan, *J. Nucl. Mater.* 69 & 70 (1978) 775.
- [11] T. Diaz de la Rubia, R.S. Averbeck and H. Hsieh, *J. Mater. Res.* 4 (1989) 579.
- [12] W.E. King and R. Benedek, *Phys. Rev.* B23 (1981) 6335.
- [13] W.E. King and R. Benedek, in: *Point Defects and Defect Interactions in Metals*, Eds. J. Takamura, M. Doyama and M. Kiritini (University of Tokyo, Tokyo, 1982) p. 807.
- [14] W.E. King and R. Benedek, *J. Nucl. Mater.* 117 (1983) 26.
- [15] M.S. Daw and M.I. Baskes, *Phys. Rev. Lett.* 50 (1983) 1285.
- [16] M.S. Daw and M.I. Baskes, *Phys. Rev.* B29 (1984) 6443.
- [17] S.M. Foiles, *Phys. Rev.* B32 (1985) 7685.
- [18] J.F. Ziegler, J.P. Biersack and U. Littmark, *The Stopping and Range of Ions in Solids* (Pergamon, New York, 1985) p. 48.
- [19] S.P. Chou and N.M. Ghoniem, University of California, Los Angeles, Report no. UCLA-Eng-9008/PPG-1257, submitted to *Phys. Rev. B* (1990).
- [20] F.F. Abraham, *Adv. Phys.* 35 (1986) 1.